DYNAMIC COMPRESSIVE RESPONSE OF PASSIVE HUMAN MUSCLES USING SPLIT HOPKINSON PRESSURE BAR

Karthikeyan Balaraman, Sudipto Mukherjee, Anoop Chawla

Department of Mechanical Engineering, Indian Institute of Technology Delhi

Rajesh Malhotra

Department of Orthopedics, All India Institute of Medical Sciences

Abstract

Development of human body models relevant to pedestrian-vehicle crash studies requires characterization of the soft tissues at strain rates up to 2000/s. Availability of properties of human muscles when loaded at such rates are limited in literature. To address this issue, a split Hopkinson pressure bar (SHPB) test setup with polymeric bars for characterizing the dynamic compressive behavior of soft tissues is presented. Use of a polymeric bar makes it possible to match impedance with human muscles. Measurements using an isolated bar tests are used to correct for the attenuation and dispersion in the waves.

Experiments are performed on human soleus and gastrocnemius muscles for strain rates ranging from ~500/s to ~1800/s. Both lower extremity muscles exhibit a concave up, nonlinear, stress-strain response at all strain rates tested. Strain rate dependency of the stress – strain response is observed. Over the strain rates tested, the soleus muscles is consistently stiffer than the

gastrocnemius muscles, and the strain rate dependence of the two muscles is similar.

DYNAMIC COMPRESSIVE RESPONSE OF PASSIVE HUMAN MUSCLES USING SPLIT HOPKINSON PRESSURE BAR

Karthikeyan Balaraman, Sudipto Mukherjee, Anoop Chawla

Department of Mechanical Engineering, Indian Institute of Technology Delhi

Rajesh Malhotra

Department of Orthopedics, All India Institute of Medical Sciences

1. Introduction

1.1. Finite element human body models for modeling pedestrian – Vehicle crashes

Pedestrian injuries constitute a significant amount of fatalities and or injuries among the all traffic users (Mohan 2004). To reduce these injuries or fatalities, pedestrian safety standards and directives are being proposed globally for the existing and new cars (Nishimoto 2003, Mizuno 2001). The pedestrian sub-system tests (legform test) may not be representative of real-world accidents because of biofidelity issues and variability in pedestrian configurations (Bhalla et al. 2003, Bose et al. 2004). Models based on finite element methods (FEM) provided with realistic geometry of human anatomy and appropriate material property of tissues would overcome these limitations. Further, a better insight of human body response under dynamic loading to enhance the safer vehicle design for pedestrians would be possible through

estimations of local stresses and strains and correlation with injury models (Mukherjee et al 2007).

At present, the viability of mimicking the human body behavior using FEM is limited by the availability of data on dynamic response of soft tissues and of suitable material models capable of representing such behavior (Chawla et al. 2006a, Chawla et al. 2006b). Muscles along with skin are the primary soft tissues which control the impact during pedestrian-vehicle crashes. During such impacts muscle acts as soft padding layer between the vehicle structure and bone, moderating the peak contact forces and the contact duration, thus altering the overall kinematics at impact. Therefore its behavior under compressive loading for different impact speeds, which translates to different strain rates, is of interest.

A methodology using SHPB test setup to characterize the soft tissue under dynamic loads is described in this paper. The response of two human lower extremity muscles for strain rates ranging from 500/s to 1800/s is presented.

1.2.   Prior data on mechanical properties of muscles

The seminal work on the material property extraction of static passive muscles dates back to the 1960's (Yamada 1970). McElhaney (1966) conducted *in vitro* dynamic tests on isolated bovine muscle for the strain rates up to 1000/s. Viscoelastic response of passive muscles of live New Zealand white rabbit subjected to tensile loads at rates less than 100/s has been reported (Best et al. 1994, Myres et al. 1998). Bosboom et al. (2001) measured the mechanical properties of rat skeletal muscle under in vivo compression loads transverse to the fiber direction. Van Sligtenhorst et al. (2006) conducted tests up to

2300/s on bovine muscle using SHPB. Song et al. (2007) characterized the porcine muscle compressive response inline as well a perpendicular to the fiber directions for strain rates ranging from 0.007/s to 3700/s. Van Loocke et al. (2008) characterized the behavior of passive porcine muscles under compression for rates from 0.5% /s to 10% /s. In a study on impact to full scale cadavers to characterize the muscle response in *in situ* conditions, Dhaliwal et al. (2002) compared the compressive response of human lower extremity muscles on volunteers, cadaveric specimens and Hybrid III dummies for low energy impact.

2. Description of split Hopkinson pressure bar tests

The split Hopkinson pressure bar (SHPB) technique uses wave propagation theory to estimate the strains and stresses for a given material. Continuous advances made in SHPB test setups have been critically reviewed by Gama et al. (2004). The SHPB experimental set-up consists of the *striker bar, incident bar* and *transmitted bar* as the main components. Schematic diagram of experimental set-up along with its components is shown in Figure 1.
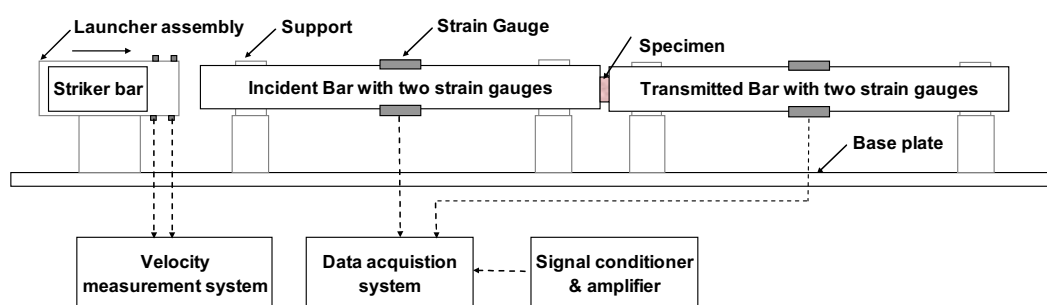

Figure 1 Schematic of set-up (Dashed line indicates electrical connections)

A thin section of the specimen is introduced between incident and transmitted bars, with the faces aligned with the bar end surfaces. The striker bar impacts the incident bar on the side opposite the specimen end. The impact initiates

pressure/stress waves that travel through the incident bar. On reaching the end, one part of it is reflected back while the other part passes through the specimen and travels to the transmitted bar. The pressure wave traveling in the incident bar, from striker bar end to specimen end, is called the *incident waves* and is compressive (See Figure 2). The strength of the tensile wave reflected back (*reflected wave*) is dependent on the relative impedance between the bar and the specimen. The compressive wave that passes through and is modified by the specimen to the transmitted bar is called the *transmitted wave*.

Impedance is defined as the ratio of the driving force F to the velocity V at a point in the bar as indicated in the equation (1)

$$Z_b = \frac{F}{V} = A_b \rho_b [C_0]_b \tag{1}$$

where Z_b is the impedance in the bar having cross sectional area as A_b with ρ_b as mass density, E_b as the Young's Modulus and $[C_0]_b$ representing the wave speed in the bar.

The relative magnitudes of the reflected and transmitted pulse with respect to the incident pulse depend upon the mechanical properties of the specimen. For good measurement, bar material with impedance of the same order as that of the specimen being tested has to be identified. Polymers such as Poly methyl metha acrylate (Z = 2.54 MPa sec / m) and Aluminum (Z = 14 MPa sec / m) alloys exhibits low impedance for similar dimensions than the steel material (Z = 41 MPa sec / m) and are used for testing soft materials (Bacon 1998, Shim et al. 2006, Chen et al. 1999, Chen et al. 2002, Song et al. 2004). More recently, (Sligtenhorst et al. 2006, Song et al. 2007), the application of

4

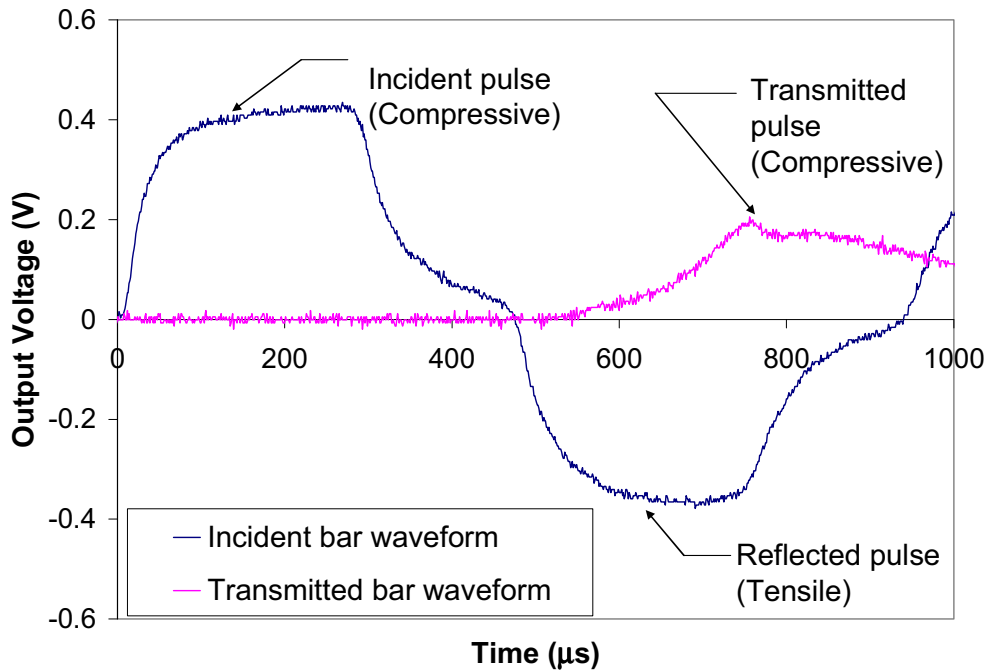SHPB tests has been extended to characterize the compressive dynamic behavior of animal muscles.

Figure 2 Typical incident bar and transmitted bar waveforms in polymeric SHPB (Reference test data: S3_T_SH_H05).

2.1. Governing equations

From one dimensional theory of elastic wave propagation, the displacement u at any time t can be related to the strain ε in the material as

$$u = C_0 \int_0^t \varepsilon \, dt \qquad (2)$$

where C_0 is the wave speed in the material.

The measure of strain corresponding to incident, reflected and transmitted waves are incident (ε_I), reflected (ε_R) and transmitted strains (ε_T) respectively. The displacement u_1, at the face of the incident bar, is the result of both the incident strain pulse ε_I traveling in the positive x direction and the

5

reflected strain pulse ε_R traveling in the negative x direction. The direction of wave propagation is as indicated in Figure 3. Thus

$$u_1 = [C_0]_{Ibar} \int_0^t \varepsilon_I \, dt + [-C_0]_{Ibar} \int_0^t \varepsilon_R \, dt = [C_0]_{Ibar} \int_0^t (\varepsilon_I - \varepsilon_R) dt \tag{3}$$
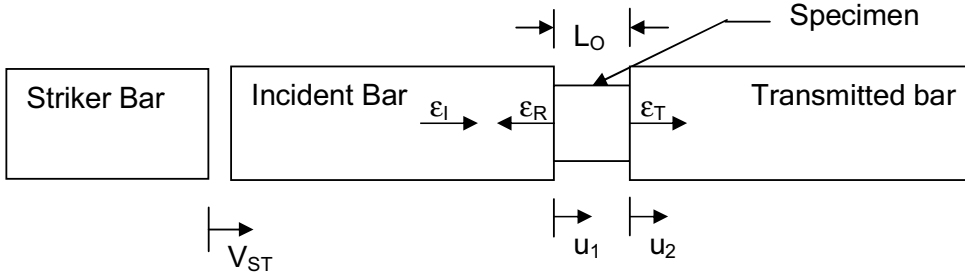

Figure 3 Schematic diagram of strain wave in the bars. Reproduced from Lindhom 1964, Fig 1. p.319

Similarly, the displacement u_2 at the face of the transmitted bar is obtained from transmitted strain pulse ε_T.

$$u_2 = [C_0]_{Tbar} \int_0^t \varepsilon_T \, dt \tag{4}$$

The nominal strain in the specimen ε_S is then calculated using equation (3) and (4) as

$$\varepsilon_S = \frac{u_1 - u_2}{L_0} = \frac{1}{L_0} \int_0^t \left([C_0]_{Ibar}(\varepsilon_I - \varepsilon_R) - [C_0]_{Tbar} \varepsilon_T\right) dt \tag{5}$$

where L_0 is the initial length of the specimen, $[C_0]_{Ibar}$ and $[C_0]_{Tbar}$ represents the wave velocity in the incident bar transmitted bar respectively.
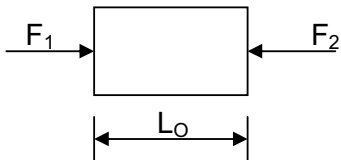

Figure 4 Free body diagram of specimen

When the bar is assumed to be elastic and using linear constitutive law $\sigma = E\varepsilon$ at both the faces result in

$$\sigma_1 = \frac{F_1}{A_{Ibar}} \text{ and } \sigma_2 = \frac{F_2}{A_{Tbar}}$$

Hence the force on the incident bar-specimen interface F_1 and specimen-transmitted bar interface F_2 are represented in terms of measured strains as

$$F_1 = A_{Ibar} E_{Ibar} (\varepsilon_I + \varepsilon_R) \tag{6}$$

$$F_2 = A_{Tbar} E_{Tbar} \varepsilon_T \tag{7}$$

where A_{Ibar}, E_{Ibar} and A_{Tbar}, E_{Tbar} represents the cross-sectional area and elastic modulus of incident and transmitted bars respectively. The free body diagram of specimen is shown in Figure 4.

Assuming that the force across the short specimen is constant,

$F_1 = F_2$, hence

$$A_{Ibar} E_{Ibar} (\varepsilon_I + \varepsilon_R) = A_{Tbar} E_{Tbar} \varepsilon_T \tag{8}$$

If the incident and transmitted bar are made from same material with equal cross sectional area, equation (8) becomes

$$\varepsilon_I + \varepsilon_R = \varepsilon_T \tag{9}$$

If both bars are of the same material, which is usually the case, $[C_0]_{Ibar} = [C_0]_{Tbar} = C_0$,

Calculation of strain, strain rate and stress in the specimen

Substituting equation (9) in equation (5), we can obtain the *nominal strain* in the specimen ε_S as

$$\varepsilon_S = \frac{C_0}{L_0} \int_0^t (-\varepsilon_R - \varepsilon_R) dt = -\frac{2C_0}{L_0} \int_0^t \varepsilon_R dt \tag{10}$$

7

Strain rate in the specimen $\dot{\varepsilon}_s$ is linearly proportional to the reflected strain

$$\dot{\varepsilon}_s = -\frac{2C_0}{L_0}\varepsilon_R \qquad (11)$$

The *average force* F_S exerted in the specimen is $F_S = \frac{F_1 + F_2}{2}$, from which the

average stress σ_S in the specimen can be calculated as

$$\sigma_S = \frac{F_S}{A_S} = \frac{F_1 + F_2}{2A_S} \qquad (12)$$

Using equation (6) and (7)

$$\sigma_S = \frac{A_{Ibar}E_{Ibar}(\varepsilon_I + \varepsilon_R) + A_{Tbar}E_{Tbar}\varepsilon_T}{2A_S} \qquad (13)$$

$$\sigma_S = \frac{A_b E_b(\varepsilon_I + \varepsilon_R + \varepsilon_T)}{2A_S} = E_b\left(\frac{A_b}{A_S}\right)\varepsilon_T \qquad (14)$$

It has to be noted that the incident, reflected and transmitted strain pulses are in practice recorded at some distance *d* away from the bar specimen interface where the stress and strain calculation is performed. The assumption of no change between the strain pulse recorded at the strain gauge mounted location and the strain pulse at the specimen-bar interface is valid when the material undergoes a linear time independent elastic deformation and geometrical effect such as radial inertia in the specimen and material effect such as the attenuation in waves during propagation are absent. When polymeric or viscoelastic bars are used then the wave attenuates (loses energy) and disperses in the medium, hence the strain measured by the strain gauges (typically at the mid location of the bar) is not the same as the strain at the specimen interface.

Corrections for attenuation and dispersion in the waves in viscoelastic bars

The quantum of dispersion and attenuation of waves vary with the *material* as well as *geometry* of the bar and it is also dependent on the frequency of the wave. The geometrical effects incorporate the influence of inertia and friction and this correction is applicable even for elastic bars. Theoretical correction in dispersion and attenuation has been generalized for viscoelastic bar by accounting for material effects (Wang et al. 1994). Subsequently, both material and geometrical effects has been addressed using generalized Pochhammer and Chree's longitudinal wave propagation equation for linear viscoelastic bars (Zhao et al. 1995) using prior knowledge of rheological material constants. Cheng et al. (1998) proposed an experimental method based on spectral analysis of wave motion for calculating the attenuation and wave numbers. Their study showed that the attenuation factors identified experimentally are nearly identical to those theoretically calculated, but the wave numbers were different due to loss of phase information during the Fast Fourier Transform (FFT) process. To find the attenuation and the propagation coefficient we use the procedure developed by Bacon (1998) which is based on an experimental methodology of computing the attenuation and wave number for any material and geometry.

In Bacon (1998), the propagation coefficient $\gamma(\omega)$ is related to the attenuation coefficient (or damping coefficient) $\alpha(\omega)$ and to the phase velocity $c(\omega)$ by

$$\gamma(\omega) = \alpha(\omega) + ik(\omega) = \alpha(\omega) + i\frac{\omega}{c(\omega)} \tag{15}$$

The attenuation coefficient $\alpha(\omega)$ and the wave number $k(\omega)$ can be derived from the amplitude $\tilde{A}_i$, and phase $\tilde{\theta}_i$, of the transfer function of the original to the decayed wave over the distance d from the free end tests. The distance d

is measured from the strain gauge location to the specimen-bar interface in the respective bars using the following expressions.

$$\alpha(\omega) = -\frac{\ln\left(\dfrac{\tilde{A}_2(\omega)}{\tilde{A}_1(\omega)}\right)}{2d} \tag{16}$$

$$k(\omega) = -\frac{\left(\tilde{\theta}_2(\omega) - \tilde{\theta}_1(\omega)\right)}{2d} \tag{17}$$

For calculating the wave number, unwrapping of phase spectra to corrects the radian phase angle by adding multiples of $\pm 2\pi$ when absolute jumps between consecutive elements are greater than π radians is needed. Phase velocity $c(\omega)$ is calculated using ratio between the angular frequency ω and wave number $k(\omega)$.

$$c(\omega) = \frac{\omega}{k(\omega)} \tag{18}$$

In viscoelastic media, the phase velocity is frequency dependent unlike in elastic analysis where it is constant for all frequencies.

Reconstruction of waves

The reflected pulse and transmitted pulse are reconstructed by incorporating attenuation and dispersion correction in the respective measured pulses over the distance it has propagated.

$$\tilde{\varepsilon}_{R\_new}(\omega) = \tilde{\varepsilon}_R(\omega) \cdot e^{\gamma d} \tag{19}$$

$$\tilde{\varepsilon}_{T\_new}(\omega) = \tilde{\varepsilon}_T(\omega) \cdot e^{\gamma d} \tag{20}$$

where $\tilde{\varepsilon}_{R\_new}(\omega)$ and $\tilde{\varepsilon}_{T\_new}$ represents reconstructed reflected and transmitted strains in frequency domain using measured reflected $\tilde{\varepsilon}_R(\omega)$ and

transmitted strain $\tilde{\varepsilon}_T(\omega)$ respectively for the distance d from the strain gauge location to the specimen-bar interface.

When viscoelastic bars are used, as the phase velocity is a function of frequency, the strain rate $\dot{\varepsilon}_S(\omega)$ in the specimen can be calculated from the reconstructed reflected strain by:

$$\dot{\varepsilon}_S(\omega) == \frac{-2 \cdot \tilde{\varepsilon}_{R\_new}(\omega)}{L_S} c(\omega) = \frac{-2 \cdot \tilde{\varepsilon}_{R\_new}(\omega)}{L_S} \left[\frac{i \cdot \omega}{\gamma(\omega)} \right] \tag{21}$$

where L_S represents the initial length of the specimen

Upon the calculation of strain rate in the specimen in time domain, strain in the specimen ε_S can be calculated by numerical integration.

$$\varepsilon_S = \int_0^t \dot{\varepsilon}_S dt \tag{22}$$

The average stress $\tilde{\sigma}_S(\omega)$ in the specimen can be calculated using the reconstructed transmitted strain $\tilde{\varepsilon}_{T\_new}$, complex Young's modulus $E^*(\omega)$, and initial cross sectional area of specimen A_S and bar A_b, using

$$\tilde{\sigma}_S(\omega) = \frac{A_b \tilde{\varepsilon}_{T\_new}(\omega)}{A_S} E^*(\omega) \tag{23}$$

The complex modulus $E^*(\omega)$ is related to the density of the bar ρ_b, frequency and propagation coefficient by:

$$E^*(\omega) = -\frac{\rho_b \omega^2}{\gamma^2(\omega)} \tag{24}$$

Substituting for $E^*(\omega)$ from equation 23 in equation 24, the average stress $\sigma_S(\omega)$ can be calculated by

$$\sigma_S(\omega) = \frac{\tilde{\varepsilon}_{T\_new}(\omega)A_b}{A_S}\left(\frac{\rho_b\omega^2}{\gamma(\omega)^2}\right) \tag{25}$$

Using inverse Fourier transform, the stresses $\sigma_S(t)$, strains $\varepsilon_S(t)$ and strain

rate $\dot{\varepsilon}_S$ can be calculated in time domain.

3. Methods

3.1. Specimen size and preparation

Tests were conducted with soleus and gastrocnemius harvested from a 43

years old male subject. Muscles were wrapped in polythene sheet and frozen

at -20 deg. C for two weeks post vitro. Subsequently, muscles were thawed at

room temperature to 20 deg. C, typically for three hours prior to testing and no

other preconditioning was done. The fascia layer is removed and measures

are taken to prevent the dehydration of the tissue during testing. Muscles

were not physically loaded till conducting the tests.

Eighteen cylindrical specimens with diameter varying from 6 to 7.5 mm and

length from 1.8 to 2.5 mm were prepared from both bulk soleus and

gastrocnemius muscles using surgical scalpels. The mean aspect ratio

(length/diameter) of the specimens obtained was 0.30±0.02 for soleus and

0.31±0.03 for gastrocnemius muscles to establish a uniform specimen

deformation, in line with earlier work (Song et al. 2007, Van Sligtenhorst

2006). The cylindrical axis of the specimen, which is the direction of loading, is

orthogonal to the fiber direction. A total of 18 tests reported here were

conducted in a 2 hour interval. Only one test was conducted on each

specimen.

3.2. Experimental setup

Both incident and transmitted bars are of Poly Metha Methyl Acrylate (PMMA) with density 1183 kg/m^3, 1000 mm long with diameter 10 mm. A 300 mm long striker bar of same diameter is launched from a spring loaded launcher mechanism. Eight foil type gauges, (1.5 mm active length, 350 ohms) are used to measure longitudinal strains in incident and transmitted bars. A Wheatstone half bridge circuit is formed with two active and two passive gauges. Active gauges are mounted diametrically opposite in the bar to measure axial strain and to counter any accidental bending. Signal conditioning amplifiers, model 2310B from Vishay micro-measurements, with inbuilt bridge excitation voltage and supporting a slew rate of 7.8 V/μs with gain of 100 and 500 was set to amplify the raw bridge output voltage measured from incident and transmitted bars respectively. We found that shielding and minimizing the lead wire length was crucial in minimizing signal noise. A two-channel oscilloscope, with inbuilt channel synchronization, (Model 54621A) from Agilent Technologies is used to record the amplified incident bar and transmitter bar strain waveforms. A time of flight optical velocity sensors fabricated in-house was used to measure the initial velocity of striker.

3.3. Experimental Protocol

A total of 18 tests were conducted targeting striker impact velocities of 2 m/s, 4 m/s and 5 m/s for both sets of muscles. Strain pulses were acquired at the rate of 1MHz for 2 milliseconds yielding 2000 data points per test. The acquisition is triggered by the incident pulse crossing a threshold value. The data acquisition is not filtered but during processing, low pass filtering for

noise reduction at around 15 kHz is used. The offline filtering was used as the cutoff is set after investigating the spectral distribution of the signal.

3.4.   Data analysis

The signal to noise (SN) ratio in the waveforms acquired from incident and transmitted bar after amplification is estimated and tests with SN ratio lower than 10 are not considered for analysis. The propagation coefficient calculation, reconstruction of waves at the specimen interface and calculation of specimen stresses, strains and strain rates using MATLAB code.

4. Results and discussion

Results: Attenuation and wave number calculation

Bacon 1998 has reported that at impact velocities in the range of 1 to 5 m/s the measured propagation coefficient does not vary significantly in polymeric bars. The coefficients from free end test at target initial velocity of 2 m/s are used in all tests. The waveform measured in the incident bar using the free end test is shown in the Figure 5. The amplitude spectra and phase spectra of the incident and reflected pulses obtained through spectral analysis are shown and Figure 6. Further, the attenuation coefficient and wave number calculated using amplitude and phase spectra respectively are shown in Figure 7 and Figure 8. The attenuation coefficient at 3, 6.8, 10.9 and 13.7 KHz which show local dips correspond to points of low signal content in the frequency spectrum of the test signal. The phase velocity calculated from the wave number at different frequencies is shown in the Figure 9. The mean phase velocity is found to be 2070 m/s for frequency up to 15 kHz and standard deviation of 25 m/s shows that influence of geometry in the existing setup is small.
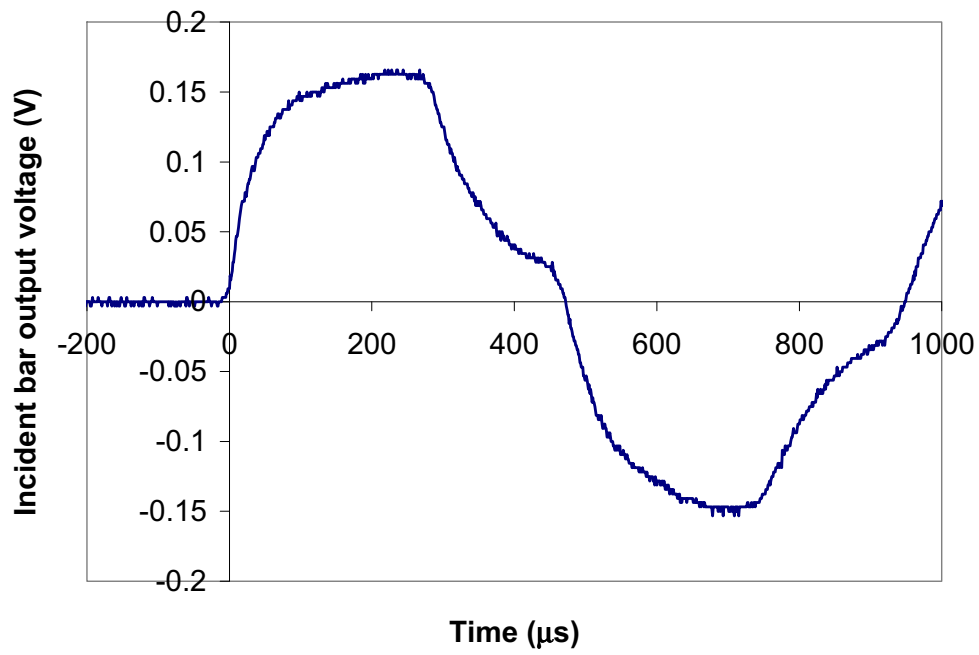
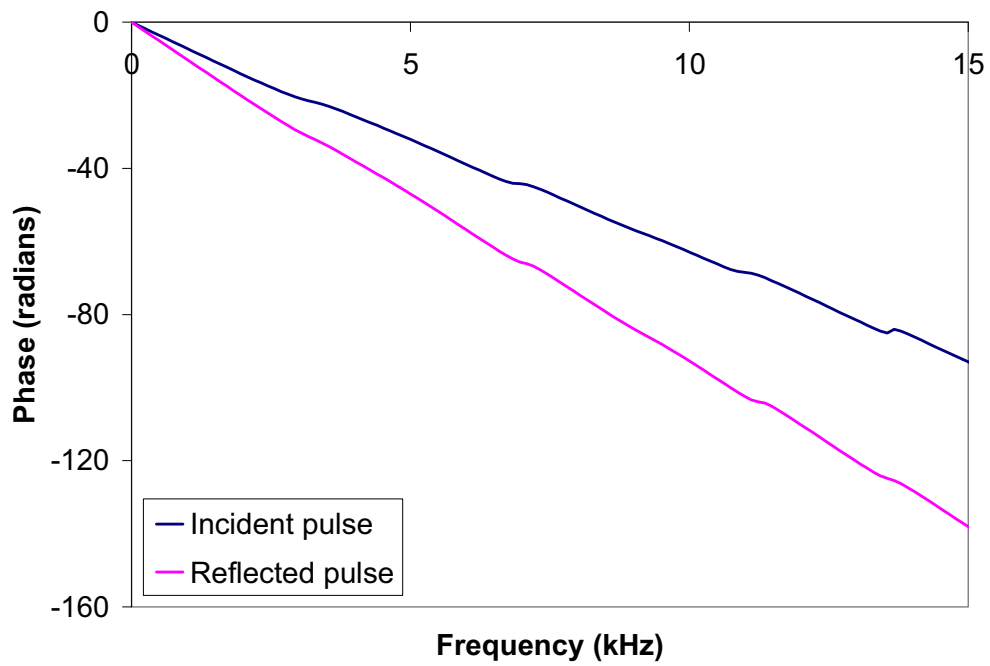**Figure 5 Incident bar wave form induced using 300 mm long striker bar for propagation coefficient calculation**
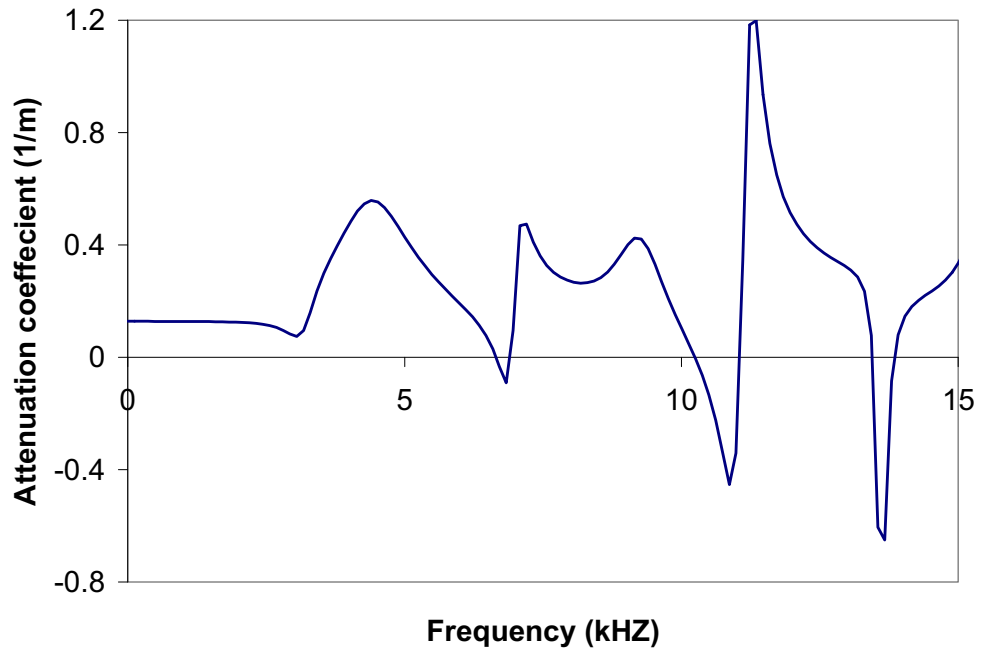
Figure 6 Phase spectrum of the incident and reflected pulse

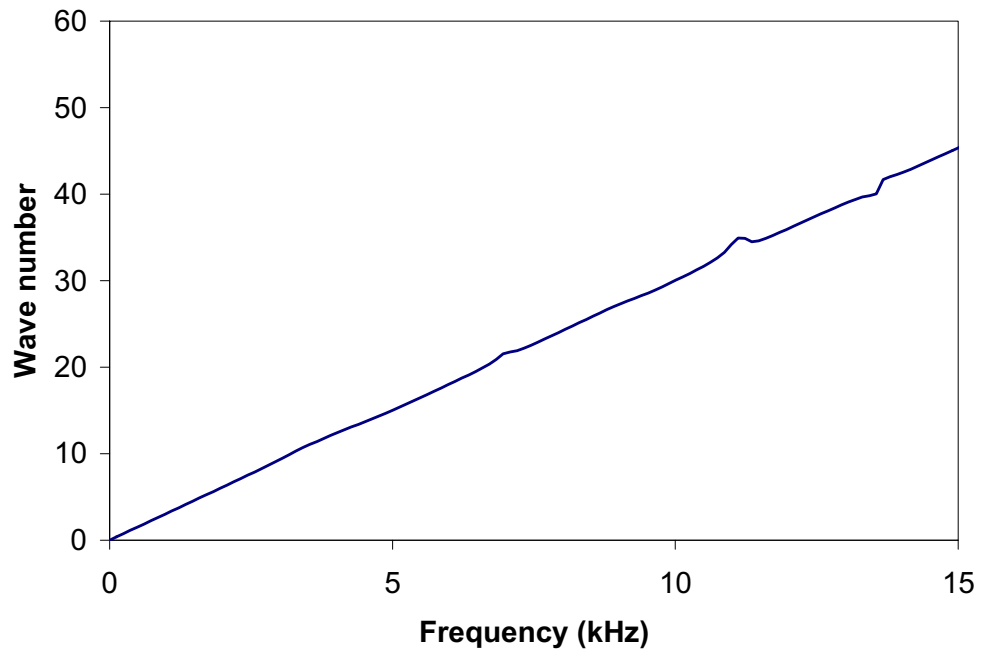**Figure 7 Attenuation coefficients for PMMA bar**
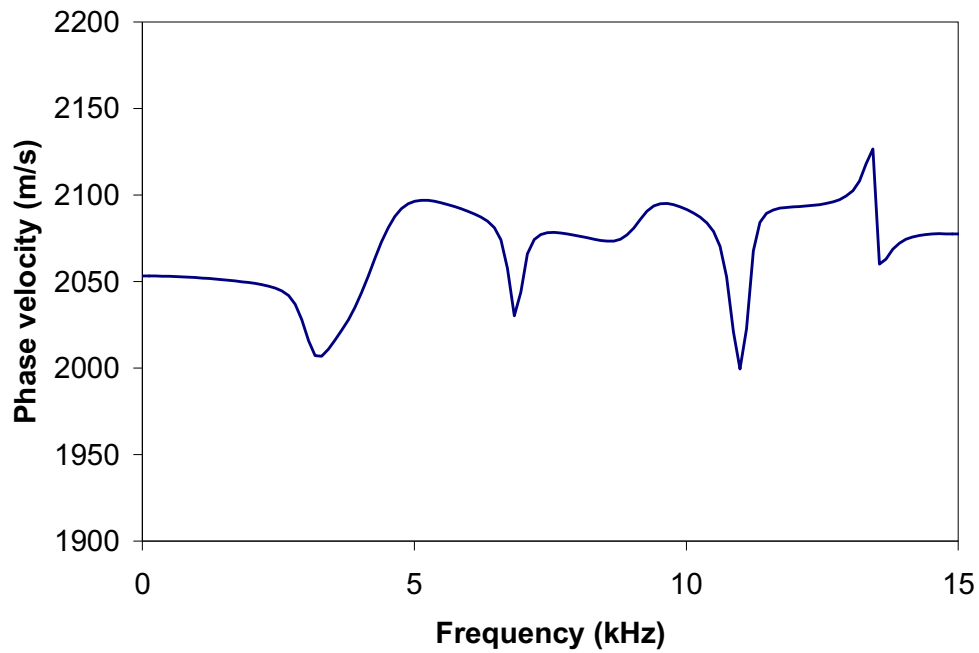

Figure 8 Wave Number for PMMA bar

Figure 9 Phase velocity for PMMA bar

Results: Stress-strain response of human lower extremity muscles

The compressive stress-strain response of human soleus and gastrocnemius muscles loaded in the direction perpendicular to the fiber orientation shows a concave-up, nonlinear, stress-strain behavior (Figure 10 and Figure 11). Strain rate dependency is evident at higher strain rates and not so around 150/s. As an overall trend, increase in strain rate increases the compressive stress measured at a particular strain in both muscles.
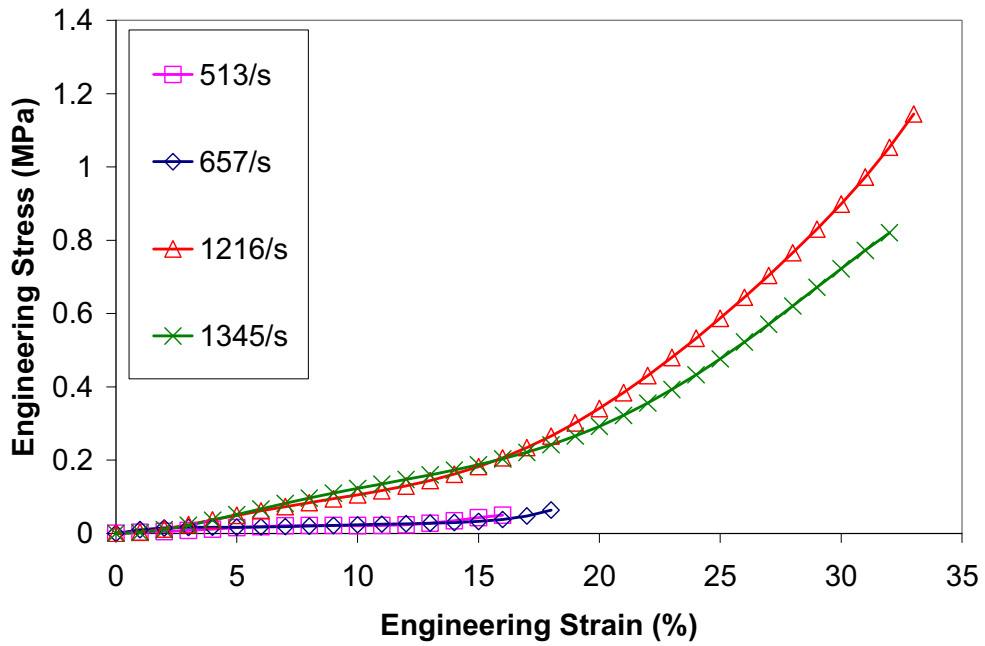
Figure 10 Stress-strain response of soleus muscle at different strain rates
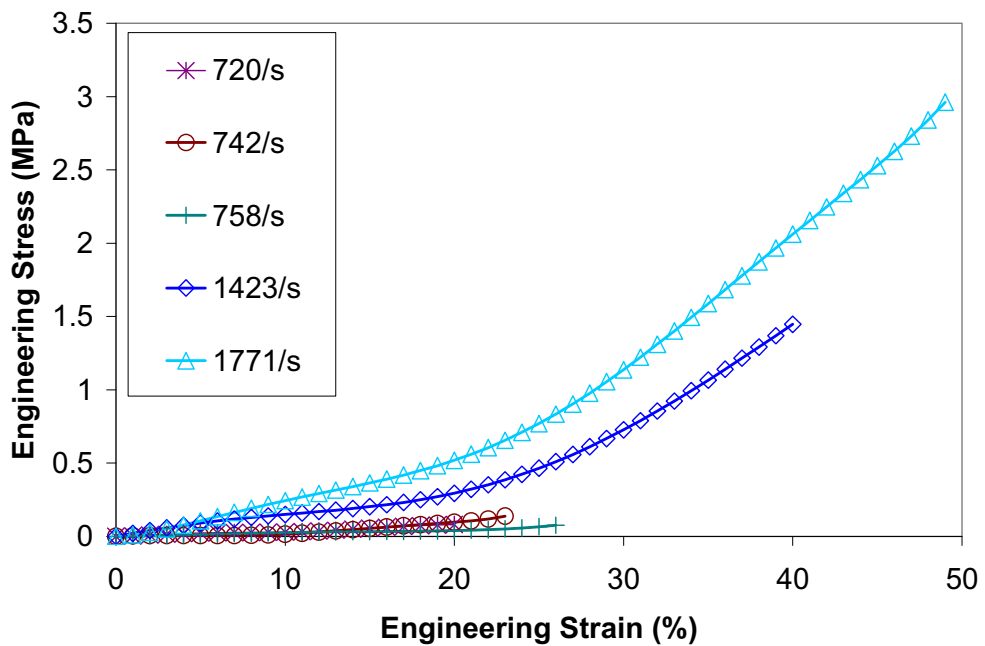

Figure 11 Stress-strain response of gastrocnemius muscle at different strain rates

Soleus muscles were found to be consistently stiffer than gastrocnemius muscle at similar strain rate as shown in Figure 12.
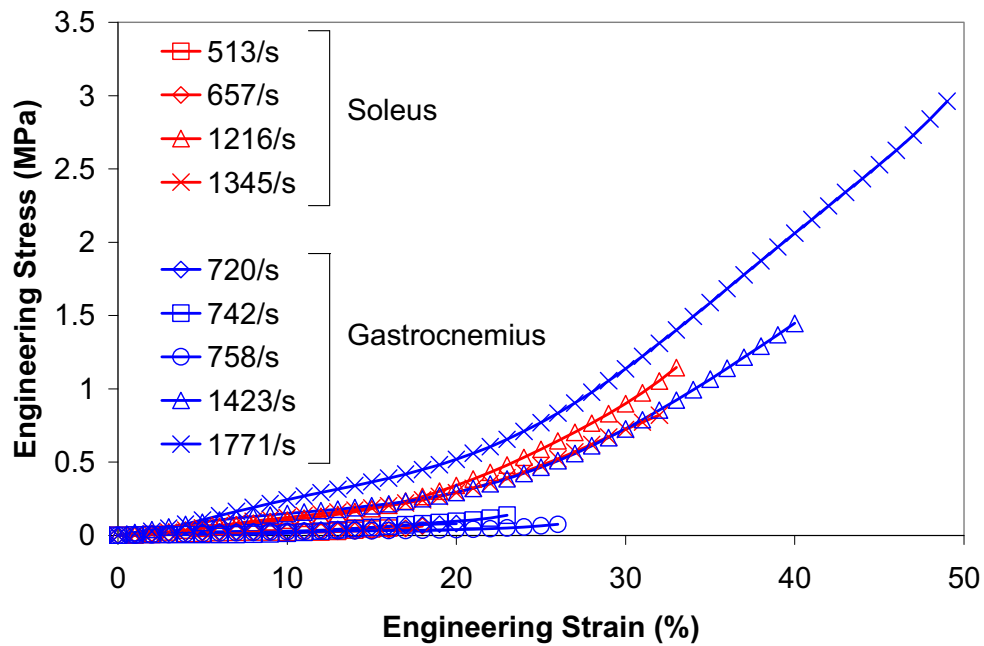
Figure 12 Comparison of dynamic stress strain response of soleus and gastrocnemius muscle

Human muscles response characterized in the present study is found to be stiffer than porcine muscle response, reported by Song et al. (2007) and bovine muscle reported by Van Sligtenhorst et al. (2006) and McElhaney (1966).

5. Conclusions

An experimental procedure using Split Hopkinson Pressure Bar (SHPB) tests and instrumentation have been established to characterize human muscle response during dynamic loading at higher strain rates. Strain rates in the range from ~500/s to ~1800/s are addressed. The developed experimental setup and methodology including the analysis procedure is repeatable and capable of measuring the stiffening effect due to strain rate response for

variation strain rates above 150/s. Use of low impedance polymeric bars for conducting tests on human muscles is demonstrated. Corrections for attenuation and dispersion during wave propagation have been incorporated using experimental methods. Two of the lower extremity muscles namely soleus and gastrocnemius are studied and differences between their responses for similar conditions are observed as preliminary results. The resulting dynamic stress-strain curves for both lower extremity muscles indicate that the material is sensitive to strain rates and the strain-rate sensitivity depends on the value of strain. Identification of a suitable constitutive model for modeling the strain rate dependent passive muscles using the muscle response obtained through the present study is needed to use the data effectively in FE models.
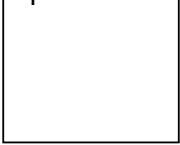
Conflict of Interests Statement

References

1. Bacon, C., 1998. An experimental method for considering dispersion and attenuation in a viscoelastic Bar, Experimental Mechanics 38, pp. 242 – 249.

2. Best, T.M., McElhaney, J., William, E.G., Myres, B.S., 1994. Characterization of the passive response of live skeletal muscle using the quasi-linear theory of viscoelasticity, Journal of Biomechanics 27, pp. 413 – 419.

3. Bhalla, K., Bose, D., Madeley, N.J., Kerrigan, J., Crandall, J., Longhitano, D., Takahashi, Y., 2003. Evaluation of the response of mechanical pedestrian knee joint impactors in bending and shear loading. In Proceedings of 18th International Technical Conference on the Enhanced Safety of Vehicle. Nagoya, Japan.

4. Bosboom, E.M.H., Hesselink, M.K.C., Oomens, C.W.J., Bouten, C.V.C., Drost, M.R., Baaijens, F.P.T., 2001. Passive transverse mechanical properties of skeletal muscle under in vivo compression. Journal of Biomechanics 34, pp. 1365–1368.

5. Bose, D., Bhalla, K., Rooij, L., Millington, S., Studley, A., Crandall, J., 2004. Response of the knee joint to the pedestrian impact loading environment. In: SAE Technical Paper Series, 2004-01-1608.

6. Chawla, A., Mukherjee, S., Karthikeyan, B., 2008. Identification of viscoelastic material properties of passive muscle tissues using genetic algorithm. Biomechanics and modeling in Mechanobiology, Article in press.

7. Chawla. A., Mukherjee, S., Karthikeyan, B., 2006a. Mechanical properties of soft tissues in the head, neck and spine. Journal of Institution of Engineers 87, pp. 3-9.

8. Chawla. A., Mukherjee, S., Karthikeyan, B., 2006b. Mechanical properties of soft tissues in the human chest, abdomen and upper extremities. Journal of Institution of Engineers, pp. 10-24.

9. Chen, W., Lu, F., Frew D.J., Forrestal M.J., 2002. Dynamic compression testing of soft materials. Journal of Applied Mechanics 69, pp. 214 – 223.

10. Chen, W., Zhang, B., Forrestal, M.J., 1999. A split Hopkinson bar technique for low-impedance materials. Experimental Mechanics 39, pp. 81–85.

11. Cheng Z.Q., Crandall J.R., Pilkey W.D., 1998. Wave dispersion and attenuation in viscoelastic split Hopkinson pressure bar. Shock and Vibration 5, pp. 307-319.

12. Dhaliwal T.S., Beillas P., Chou C.C., Prasad P., Yang K.H., King A.I., 2002. Structural response of lower leg muscles in compression: a low impact energy study employing volunteers, cadavers and the Hybrid III. Stapp Car Crash Journal 46, pp. 229–243.

13. Gama B.A., Lopatnikov S.L., Gillespie Jr J.W., 2004. Hopkinson bar experimental technique: A critical review. Applied Mechanics Reviews 57, pp. 223-250.

14. Karthikeyan, B., Mukherjee, S., Chawla, A., Malhotra R., 2006. Soft tissue characterization for compressive loading using experiments and finite element methods. SAE 2006 Transactions Journal of Passenger Cars-Mechanical Systems 115, pp. 173–182.

15. Lindhom, U.S., 1964. Some experiments with the split Hopkinson pressure bar. Journal of the Mechanics and Physics of Solids 1964, pp. 317 – 335.

16. McElhaney, J., 1966. Dynamic response of bone and muscle tissue. Journal of Applied Physiology 21, pp. 1231 – 1236.

17. Miller, K., 2002. Mechanical properties of brain tissue in tension. Journal of Biomechanics 35, pp. 483 – 490.

18. Mizuno, Y., 2003. Summary of IHRA pedestrian safety WG activities (2003) – proposed test methods to evaluate pedestrian protection afforded

by passenger cars. In Proceedings of 18th International Technical Conference on the Experimental Safety of Vehicles. Nagoya, Japan.

19. Mohan, D., 2004. Road traffic deaths and injuries in India: time for action. The national medical journal of India 17, pp. 63 – 66.

20. Mukherjee, S., Chawla, A., Karthikeyan, B., Soni A., 2007. Finite element crash simulations of the human body: passive and active muscle modeling. Sadhana-Academy Proceedings in Engineering Sciences 32, pp. 409–426.

21. Myres, B.S., Woolley, C.T., Slotter, T. L., Garrett, W.E., Best, T.M., 1998. The influence of strain rate on the passive and stimulated engineering stress-large strain behavior of the rabbit tibialis anterior muscle. Journal of Biomechanical Engineering 120, pp.126 – 132.

22. Nishimoto, T., 2003. Introduction of the regulation of pedestrian head protection in Japan. In Proceedings of 18th international conference on the enhanced safety vehicles. Nagoya, Japan.

23. Salisbury, C., 2001. Spectral analysis of wave propagation through a polymeric Hopkinson bar. Master of Science Thesis, Mechanical Engineering Department, University of Waterloo, Ontario.

24. Shim V.P.W., Liu J.F., Lee V.S., 2006. A technique for dynamic tensile testing of human cervical spine ligaments. Experimental Mechanics 46, pp. 77– 89.

25. Song, B., Chen. W., Ge, Y., Weerasooriya, T., 2007. Dynamic and quasi-static compressive response of porcine muscle. Journal of Biomechanics 40, pp. 2999 – 3005.

26. Song, B., Chen, W., 2004. Dynamic stress equilibration in split Hopkinson pressure bar tests on soft materials. Experimental Mechanics 44, pp. 300-312.

27. Van Loocke, M., Lyons, C.G., Simms, C.K., 2008. Viscoelastic properties of passive skeletal muscle in compression: Stress-relaxation behaviour and constitutive modeling. Journal of Biomechanics 41, pp. 1555 – 1566.

28. Van Sligtenhorst, C., Cronin, D.S., Brodland, G.W., 2006. High strain rate compressive properties of bovine muscle tissue determined using a split Hopkinson bar apparatus. Journal of Biomechanics 39, pp.1852– 1858.

29. Wang, L., Labibes, K., Azari, Z., Pluvinage, G., 1994. Generalization of split Hopkinson bar technique to use viscoelastic bars. International Journal of Impact Engineering 15, pp. 669 – 686.

30. Yamada, H., 1970. Strength of biological materials. The Williams & Wilkins Company, Baltimore

31. Zhao, H., Gary, G., 1995. A three dimensional analytical solution of the longitudinal wave propagation in an infinite linear viscoelastic cylindrical bar: Application to experimental techniques. Journal of the Mechanics and Physics of Solids, 43, pp. 1335 – 1348.